On the detection of the imprints of primordial gravitational waves on the CMB by BICEP2

L. Sriramkumar

Department of Physics, Indian Institute of Technology Madras, Chennai

Institute of Mathematical Sciences, Chennai

March 21, 2014

Plan of the talk

1. The Cosmic Microwave Background (CMB)
2. Anisotropies in the CMB, polarization, and the angular power spectra
3. Perturbations in the early universe and imprints on the CMB
4. The results from BICEP2
5. The inflationary paradigm
6. Confronting inflationary power spectra with the CMB data
7. Summary

A few words on the conventions and notations

- We shall work in units such that $c = \hbar = 1$, and define the Planck mass to be $\mathrm{M}_{\mathrm{Pl}} = (8\,\pi\,G)^{-1/2}$.
- As is often done, particularly in the context of inflation, we shall assume the background universe to be described by the spatially flat, Friedmann line-element.
- We shall denote differentiation with respect to the cosmic and the conformal times t and η by an overdot and an overprime, respectively.
- Moreover, N shall denote the number of e-folds.
- Further, as usual, a and $H = \dot{a}/a$ shall denote the scale factor and the Hubble parameter associated with the Friedmann universe.
- Lastly, note that $\mathrm{M}_{\mathrm{Pl}} \simeq 2.4 \times 10^{18}\,\mathrm{GeV}$.

The spectrum of the CMB

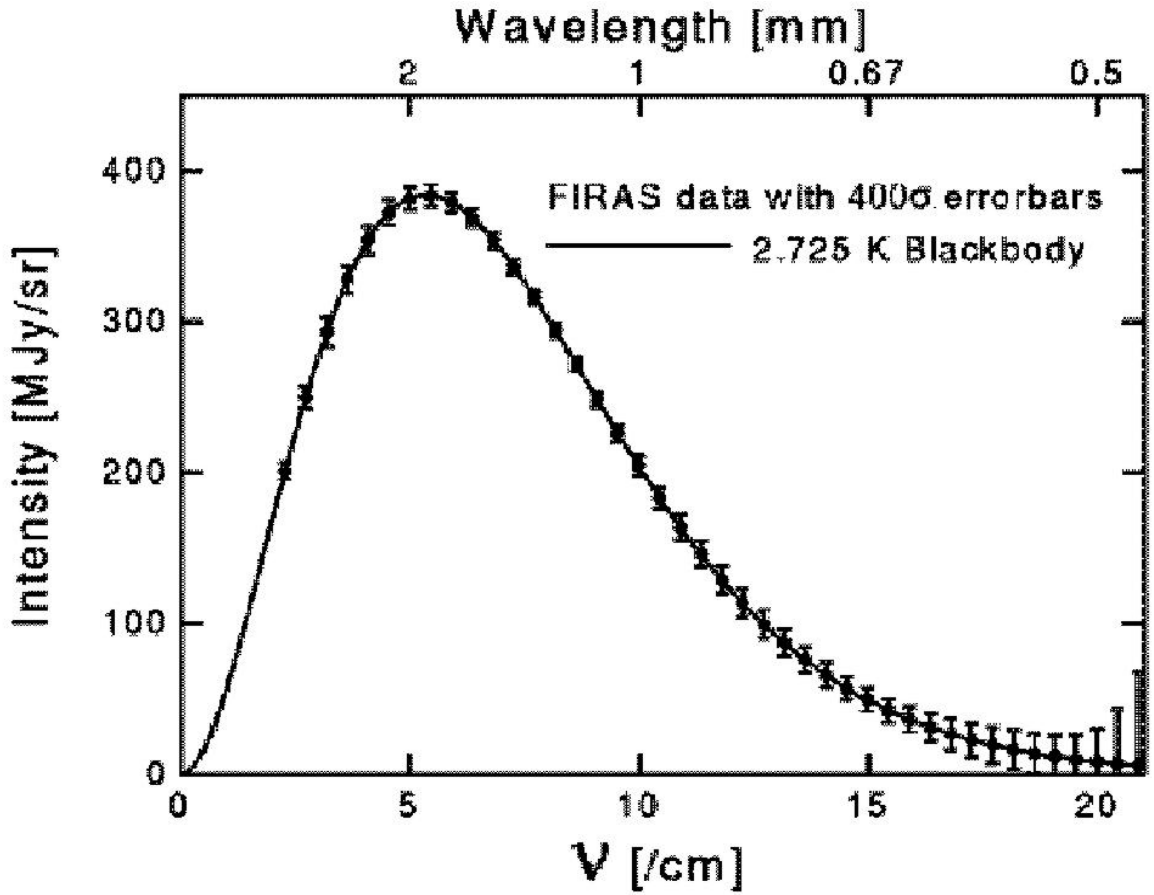

The spectrum of the CMB as measured by the COBE satellite[1]. It is such a perfect Planck spectrum (corresponding to a temperature of 2.725° K) that it is unlikely to be bettered in the laboratory. The error bars in the graph above have been amplified 400 times so that they can be seen!

[1] Image from http://www.astro.ucla.edu/~wright/cosmo_01.htm.

The timeline of the universe

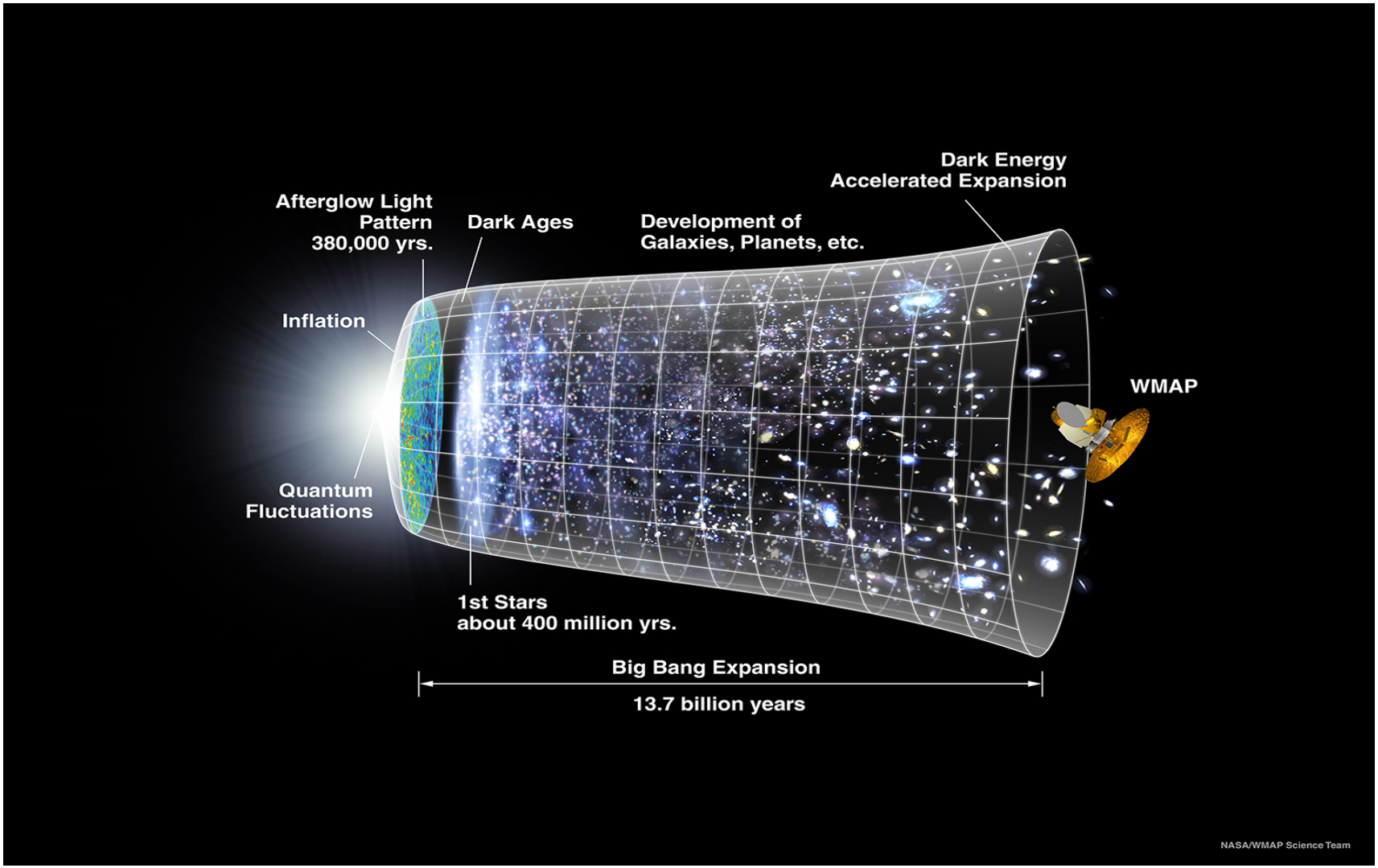

A pictorial timeline of the universe – from the big bang until today[2].

[2] See http://wmap.gsfc.nasa.gov/media/060915/060915_CMB_Timeline150.jpg.

Decoupling of matter and radiation[3]

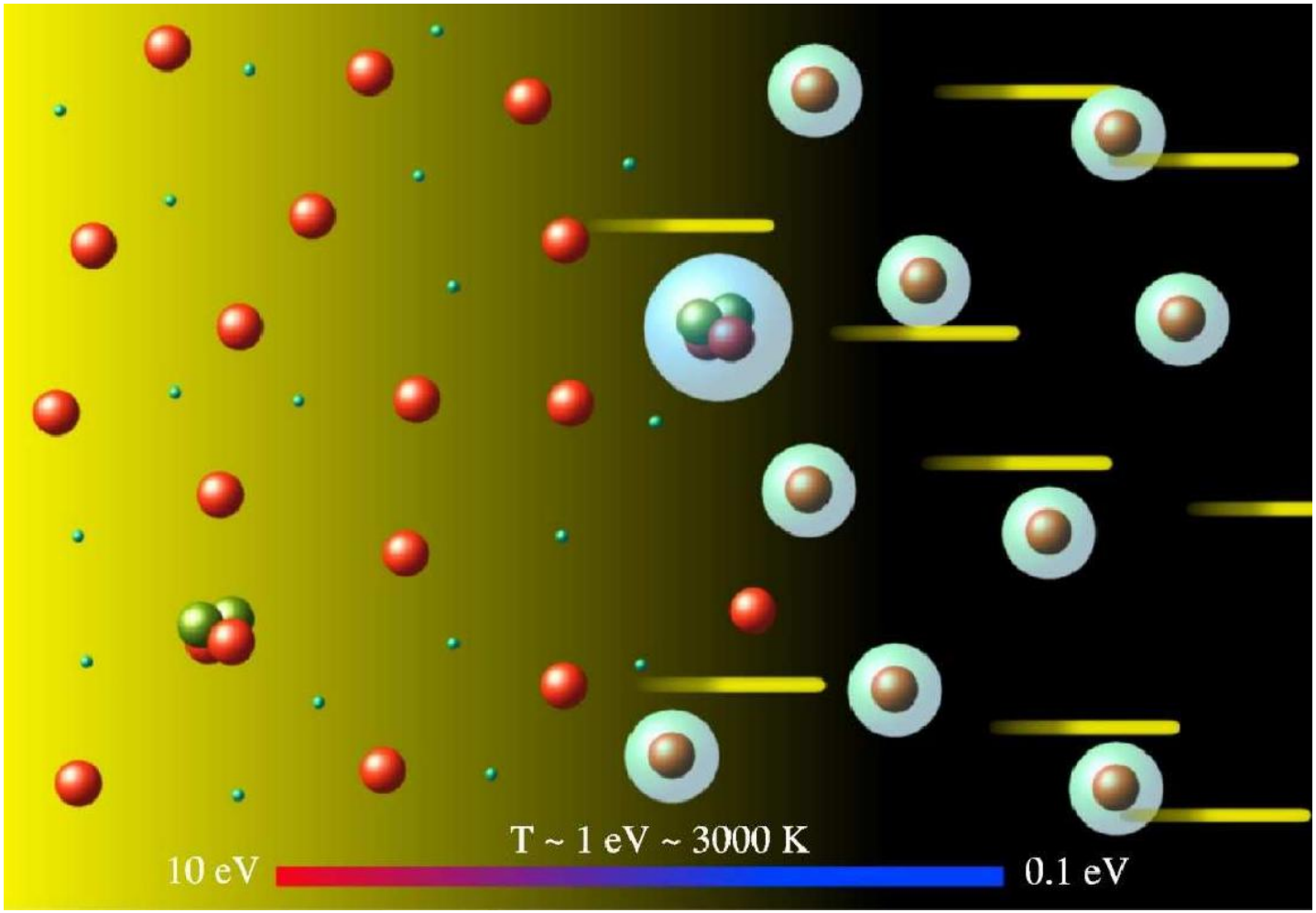

Radiation ceases to interact with matter at a temperature of about $T \simeq 3000^{\circ}\ \mathrm{K}$, which corresponds to a red-shift of about $z \simeq 1000$.

[3] Image from W. H. Kinney, arXiv:astro-ph/0301448v2.

CMB anisotropies as seen by WMAP and Planck

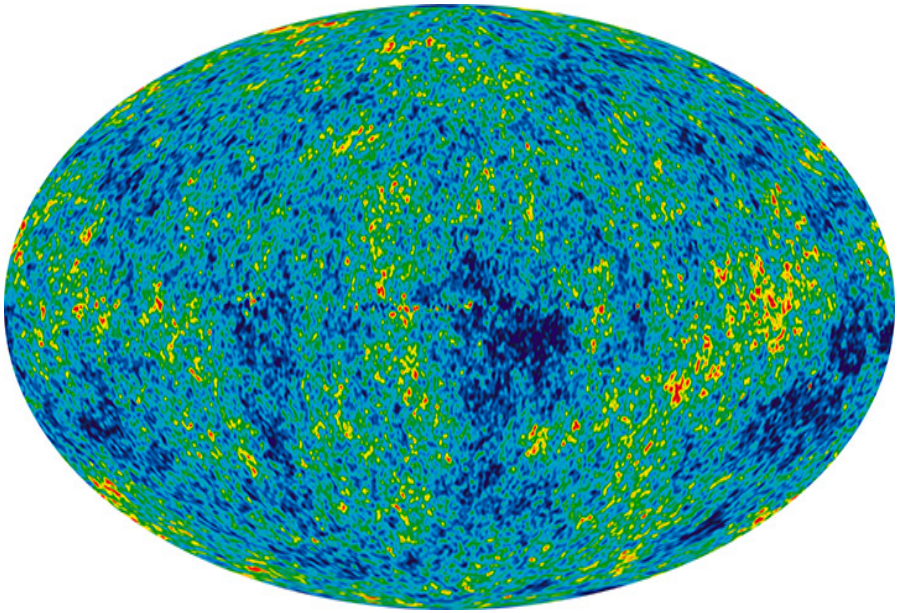

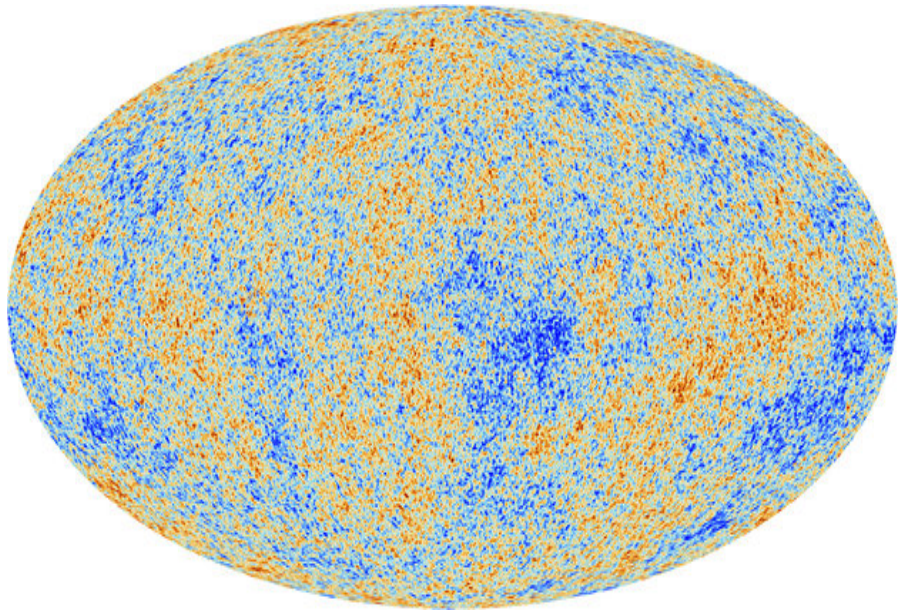

Left: All-sky map of the anisotropies in the CMB created from nine years of Wilkinson Microwave Anisotropy Probe (WMAP) data[4].

Right: The CMB anisotropies as observed by the more recent Planck mission[5]. The above images show temperature variations (as color differences) of the order of $200^\circ\ \mu\mathrm{K}$. The angular resolution of WMAP was about 1°, while that of Planck was a few arc minutes. These temperature fluctuations correspond to regions of slightly different densities, and they represent the seeds of all the structure around us today.

[4] Image from http://wmap.gsfc.nasa.gov/media/121238/index.html.

[5] Image from http://www.esa.int/Our_Activities/Space_Science/Planck/Planck_reveals_an_almost_perfect_Universe.

Polarization of the CMB[6]

The radiation in the CMB is expected to be polarized because of Compton scattering (actually, Thomson scattering) at the time of decoupling.

Moreover, Compton scattering produces polarization only when the incident field has a quadrupole moment. But, the tight coupling between the electrons and the photons before decoupling leads to only a small quadrupole. This, in turn, implies that the signal in the polarization is expected to be much smaller than the anisotropies themselves.

It should be noted that Compton scattering leads to linear polarization.

Apart from Compton scattering at the epoch of decoupling, the CMB photons are also polarized by weak gravitational lensing due to the intervening clustered matter, as they propagate towards us.

[6] See, for instance, S. Dodelson, *Modern Cosmology* (Academic Press, San Diego, 2003), Sec. 10.4.

Polarization and the Stokes' parameters[7]

Recall that, a propagating, plane and monochromatic electromagnetic wave will, in general, be elliptically polarized.

Such a polarized wave is often described in terms of the so-called Stokes' parameters Q, U and V, with the intensity, say, I, of the radiation being given by $I^2 = Q^2 + U^2 + V^2$.

In general, the radiation will be elliptically polarized, with V characterizing the circularity parameter that measures the ratio of the principal axes of the ellipse. The wave is said to have left-or-right handed polarization, if V is positive or negative, with a vanishing V corresponding to linear polarization.

The parameters Q or U determine the orientation of the ellipse.

[7] See, for instance, G. B. Rybicki and A. P. Lightman, *Radiative Processes in Astrophysics* (Wiley-Interscience, New York, 1979), Sec. 2.4.

The E and the B modes of polarization[8]

In the case of linear polarization, we require only the parameters Q and U to characterize the electromagnetic wave.

These two parameters can be thought of as the components of a symmetric and trace-free, second rank tensor, and expressed in terms of two new quantities, say, E and B, as follows:

$$\begin{pmatrix} Q & U \\ U & -Q \end{pmatrix} \propto \left(\partial_i\,\partial_j - \frac{1}{2}\,\delta_{ij}\,\nabla^2\right) E + \epsilon_{k\,(i}\partial_{j)}\partial_k\,B.$$

Essentially, the two-dimensional vector describing the linearly polarized electromagnetic wave has been decomposed, using the conventional Helmholtz theorem, into a part involving the gradient of a scalar (*viz.* E) and a divergence free part, involving the curl (*viz.* B)

Evidently, while E is a scalar, B is a pseudo-scalar.

[8] See, for instance, A. Challinor, arXiv:1210.6008 [astro-ph.CO].

Illustration of the E and the B modes[9]

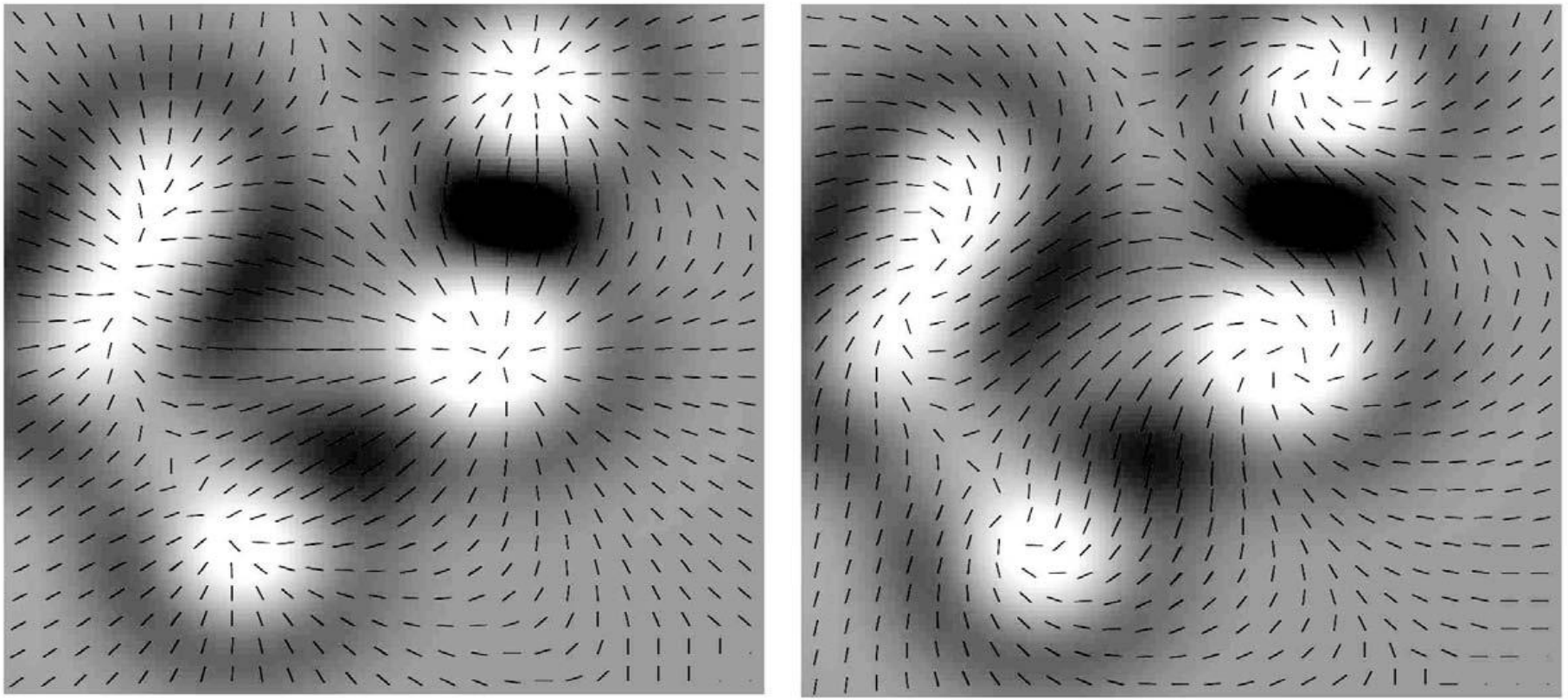

An illustration of the E (on the left) and B (on the right) types of polarization.

[9] Images from, R. Durrer, *The Cosmic Microwave Background* (Cambridge University Press, Cambridge, England, 2008), p. 196.

The definition of the CMB angular power spectrum[10]

The deviation from the mean value of the CMB temperature in a given direction of the sky, say $\hat{\boldsymbol{n}}$, can be expanded in terms of the spherical harmonics as follows:

$$\frac{\Delta T\left(\hat{\boldsymbol{n}}\right)}{T} = \sum_{\ell=2}^{\infty} \sum_{m=-\ell}^{m=\ell} a_{\ell m} Y_{\ell m}\left(\hat{\boldsymbol{n}}\right).$$

The correlation function of the deviations is defined as

$$C(\theta) \equiv \left\langle \left[\Delta T\left(\hat{\boldsymbol{n}}_1\right)\, \Delta T\left(\hat{\boldsymbol{n}}_2\right)\right]/T^2 \right\rangle,$$

where $\cos\theta = \hat{\boldsymbol{n}}_1 \cdot \hat{\boldsymbol{n}}_2$ and the average is taken across all the pairs of points in the sky.

As there is no preferred direction, we have $\left\langle a^*_{\ell m}\, a_{\ell' m'} \right\rangle = C_\ell\, \delta_{\ell\ell'}\, \delta_{mm'}$ so that

$$C(\theta) = \frac{1}{4\,\pi} \sum_{l=2}^{\infty} \left(2\,\ell + 1\right)\, C_\ell\, P_\ell\left(\cos\theta\right),$$

where $P_\ell\left(\cos\theta\right)$ are the Legendre polynomials and C_ℓ are the observed quantities known as the multipole moments.

[10] See, for example, S. Weinberg, *Cosmology* (Oxford University Press, Oxford, England, 2008), Sec. 2.6.

The character of the perturbations

In a Friedmann universe, the perturbations in the metric and the matter can be classified according to their behavior with respect to local rotations of the spatial coordinates on hypersurfaces of constant time as follows[11]:

- Scalar perturbations – Density and pressure perturbations
- Vector perturbations – Rotational velocity fields
- Tensor perturbations – Gravitational waves

The metric perturbations are related to the matter perturbations through the first order Einstein's equations.

The scalar perturbations leave the largest imprints on the CMB, and are primarily responsible for the inhomogeneities in the distribution of matter in the universe.

In the absence of sources, vector perturbations decay rapidly in an expanding universe.

Whereas, the tensor perturbations, *i.e.* the gravitational waves, can be generated even in the absence of sources.

[11] See, for instance, L. Sriramkumar, Curr. Sci. **97**, 868 (2009).

The primordial perturbation spectra[12]

When comparing with the observations, for simplicity, one often uses the following power law, template scalar and tensor spectra:

$$\mathcal{P}_{\rm S}(k) = \mathcal{A}_{\rm S}\left(\frac{k}{k_*}\right)^{n_{\rm S}-1} \quad \text{and} \quad \mathcal{P}_{\rm T}(k) = \mathcal{A}_{\rm T}\left(\frac{k}{k_*}\right)^{n_{\rm T}},$$

where $\mathcal{A}_{\rm S}$ and $\mathcal{A}_{\rm T}$ denote the scalar and tensor amplitudes, k_* represents the so-called pivot scale at which the amplitudes are quoted, while the spectral indices $n_{\rm S}$ and $n_{\rm T}$ are assumed to be constant.

The tensor-to-scalar ratio r is defined as

$$r(k) \equiv \frac{\mathcal{P}_{\rm T}(k)}{\mathcal{P}_{\rm S}(k)}$$

and, often, the dependence of r on the wavenumber of k is assumed to be very weak.

[12] See, for instance, L. Sriramkumar, Curr. Sci. **97**, 868 (2009).

Theoretical angular power spectra[13]

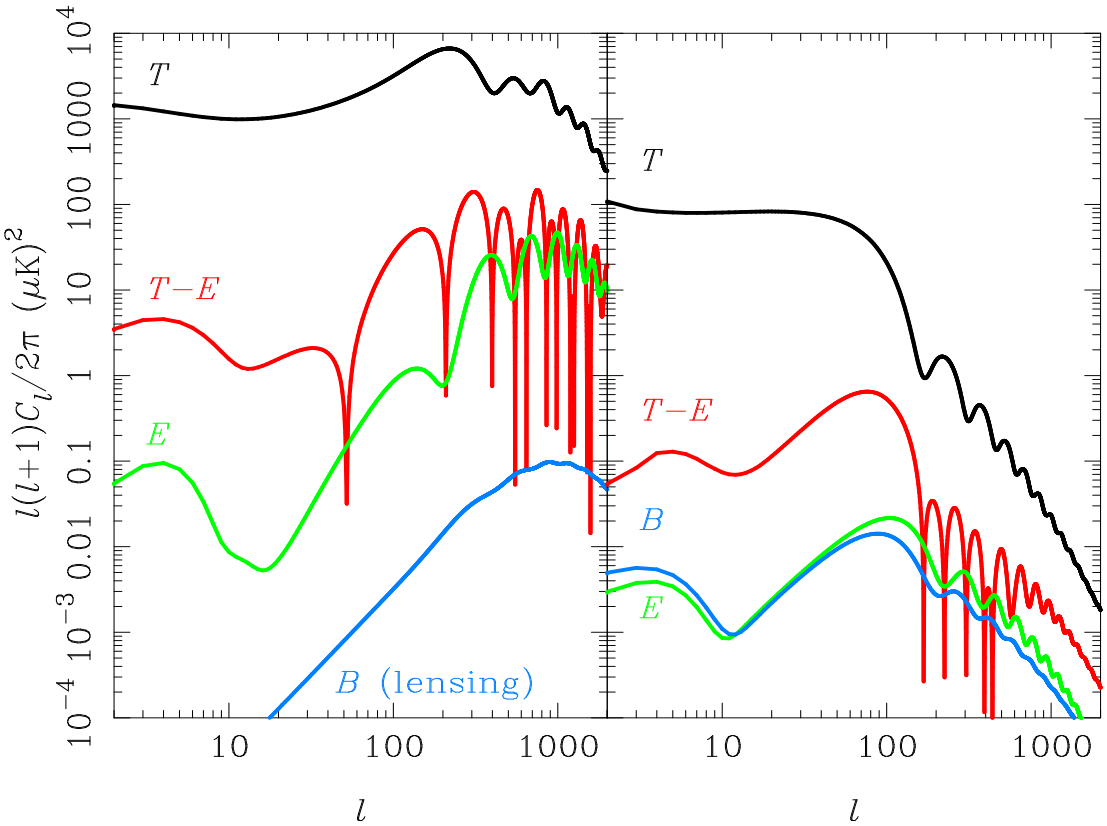

The different *theoretically* computed, CMB angular power and cross-correlation spectra – temperature (T) in black, E in green, B in blue, and T-E in red – arising due to scalars (on the left) and tensors (on the right) corresponding to a tensor-to-scalar ratio of $r = 0.24$. The B-mode spectrum induced by weak gravitational lensing has also been shown (in blue) in the panel on the left.

[13] Figure from, A. Challinor, arXiv:1210.6008 [astro-ph.CO].

TT angular power spectrum from the WMAP data[14]

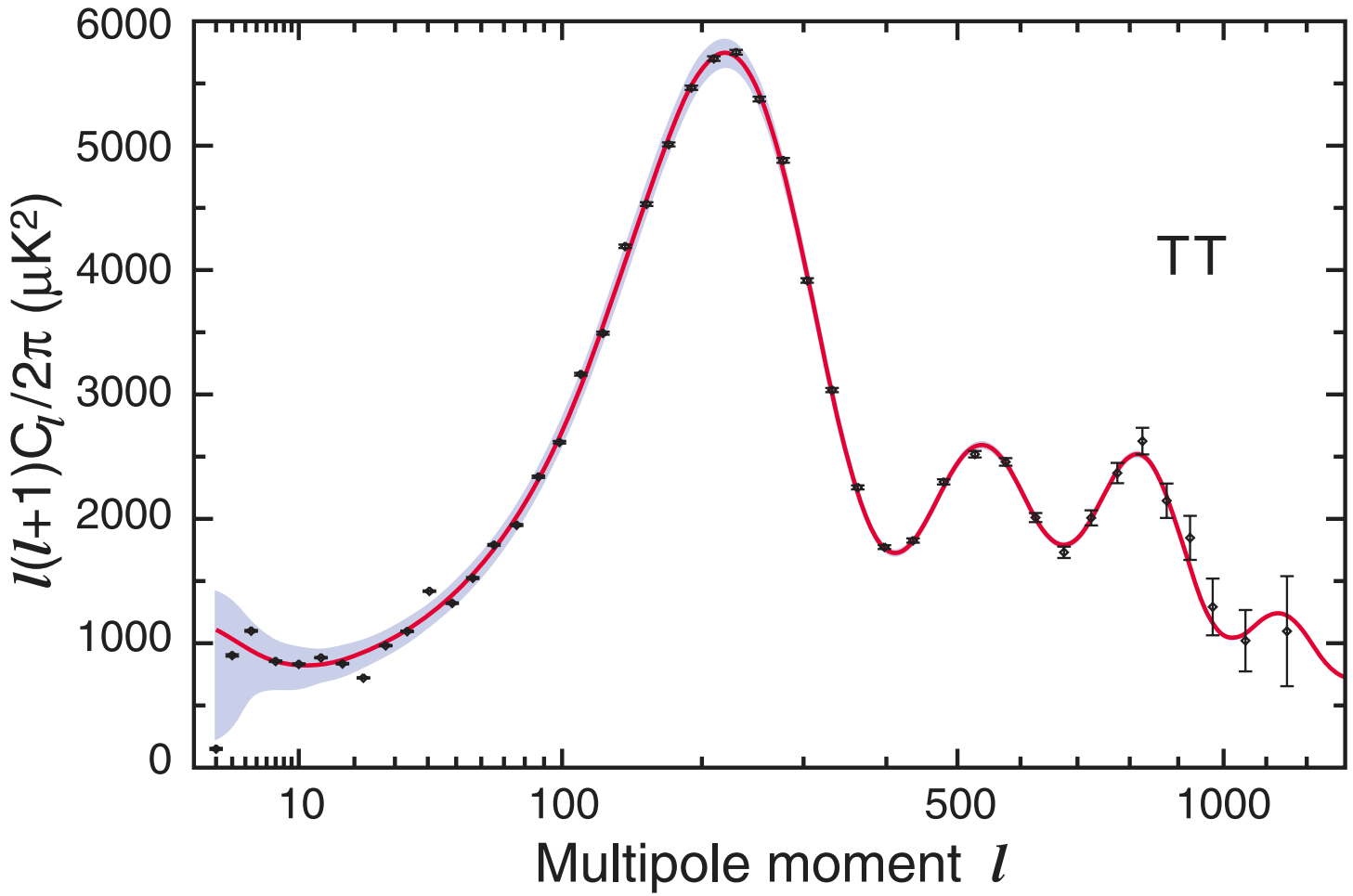

The WMAP 9-year data for the CMB TT angular power spectrum (the black dots with error bars) and the theoretical, best fit ΛCDM model with a power law primordial spectrum (the solid red curve).

[14] C. L. Bennett *et al.*, Astrophys. J. Suppl. **208**, 20 (2013).

TT angular power spectrum from the Planck data[15]

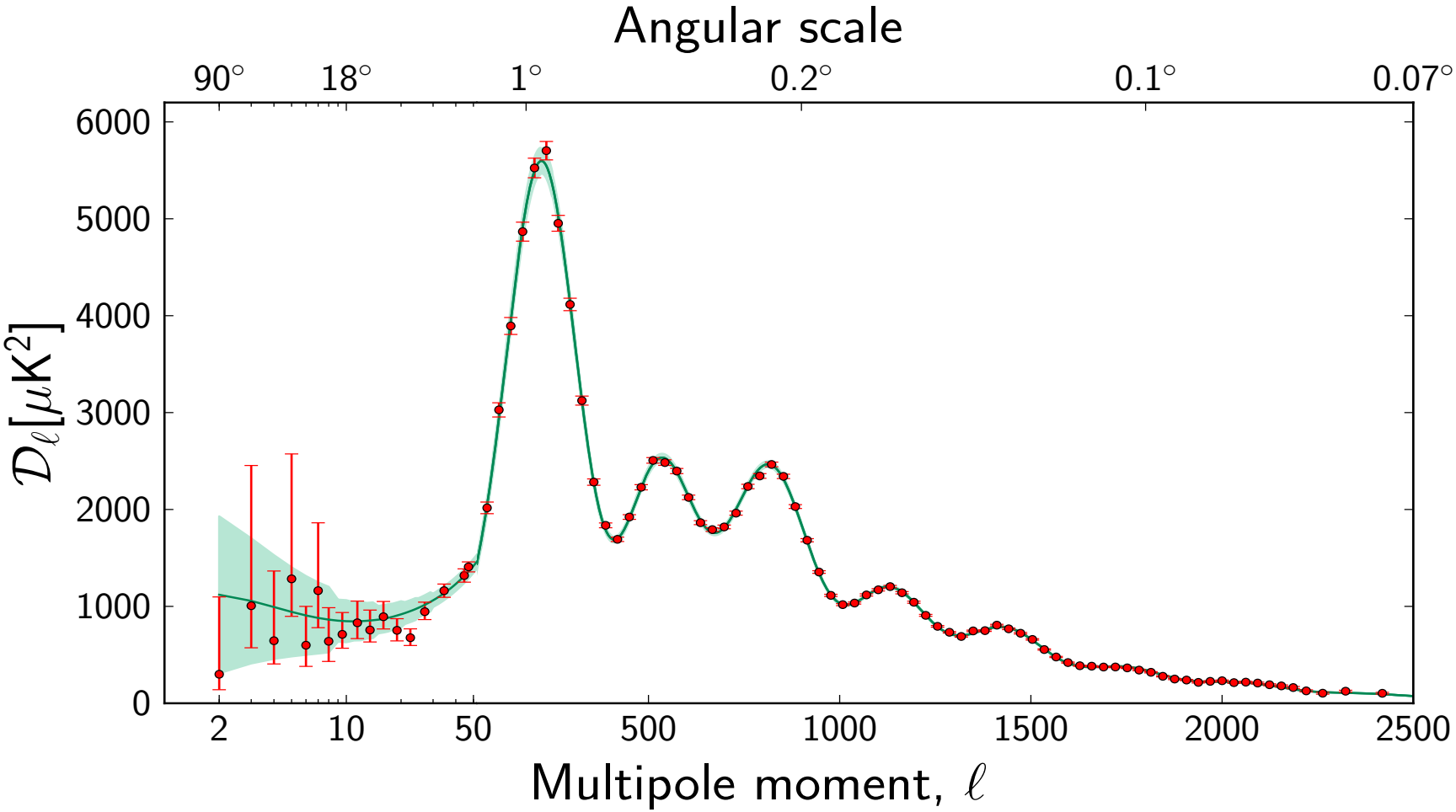

The CMB TT angular power spectrum from the Planck data (the red dots with error bars) and the best fit ΛCDM model with a power law primordial spectrum (the solid green curve).

[15] P. A. R. Ade *et al.*, arXiv:1303.5075 [astro-ph.CO].

The observed polarization angular power spectra[16]

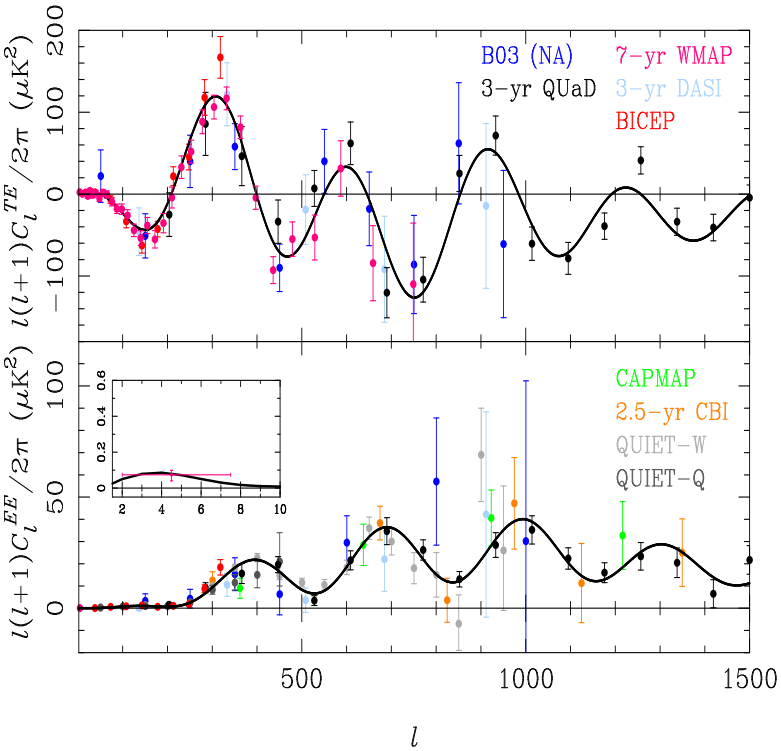

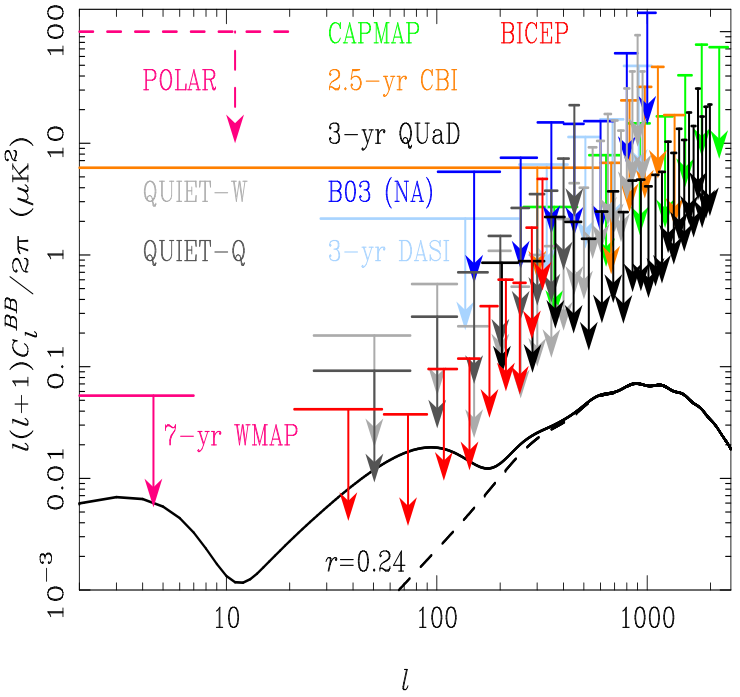

Measurements and lower bounds on the CMB polarization angular power and cross-correlation spectra by different CMB missions, prior to BICEP2.

[16] Figure from, A. Challinor, arXiv:1210.6008 [astro-ph.CO].

The BICEP2 instrument at the south pole

The BICEP2[17] instrument that had operated at the south pole from January 2010 through December 2012.

[17] Image from http://www.cfa.harvard.edu/CMB/bicep2/.

The observing fields of BICEP2[18]

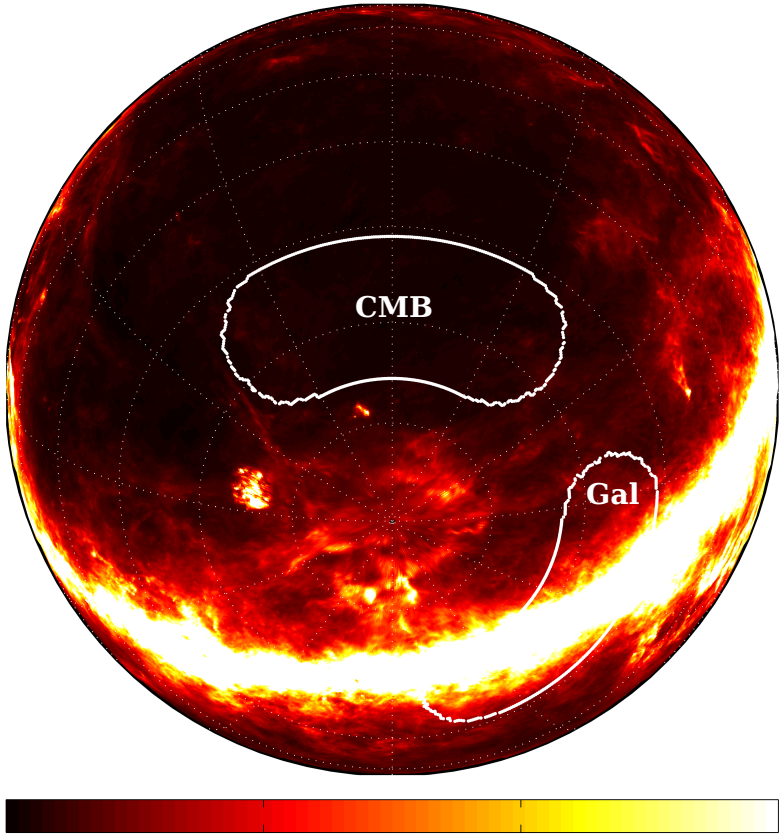

BICEP2 observes the CMB at the frequency of $150\,\mathrm{GHz}$ mostly in a field of about $1000\,\mathrm{deg}^2$ (*i.e.* about 2.4% of the sky) in the so-called 'southern hole'. The southern hole lies away from the galactic plane, where polarized foregrounds (as shown above) are expected to be especially low.

[18] P. A. R. Ade *et al.*, arXiv:1403.4302 [astro-ph.CO].

The E and B modes observed by BICEP2[19]

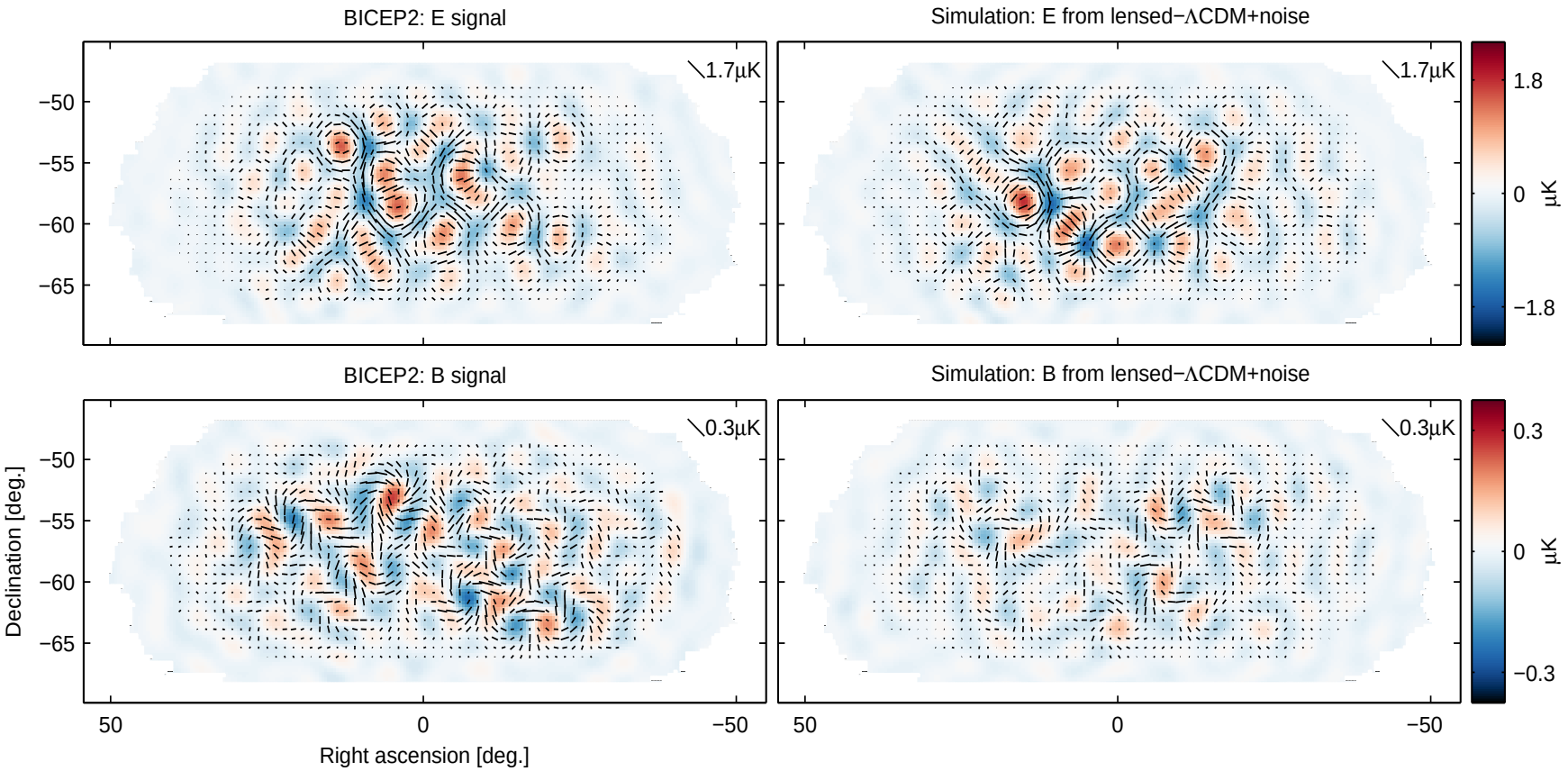

Maps of E and B modes from BICEP2 (on the left) and equivalent maps (on the right) that have been simulated. The color scale displays the E-mode scalar and B-mode pseudo-scalar patterns, while the lines represent the equivalent magnitude and orientation of linear polarization.

[19] P. A. R. Ade *et al.*, arXiv:1403.4302 [astro-ph.CO].

The detection of the B mode polarization by BICEP2

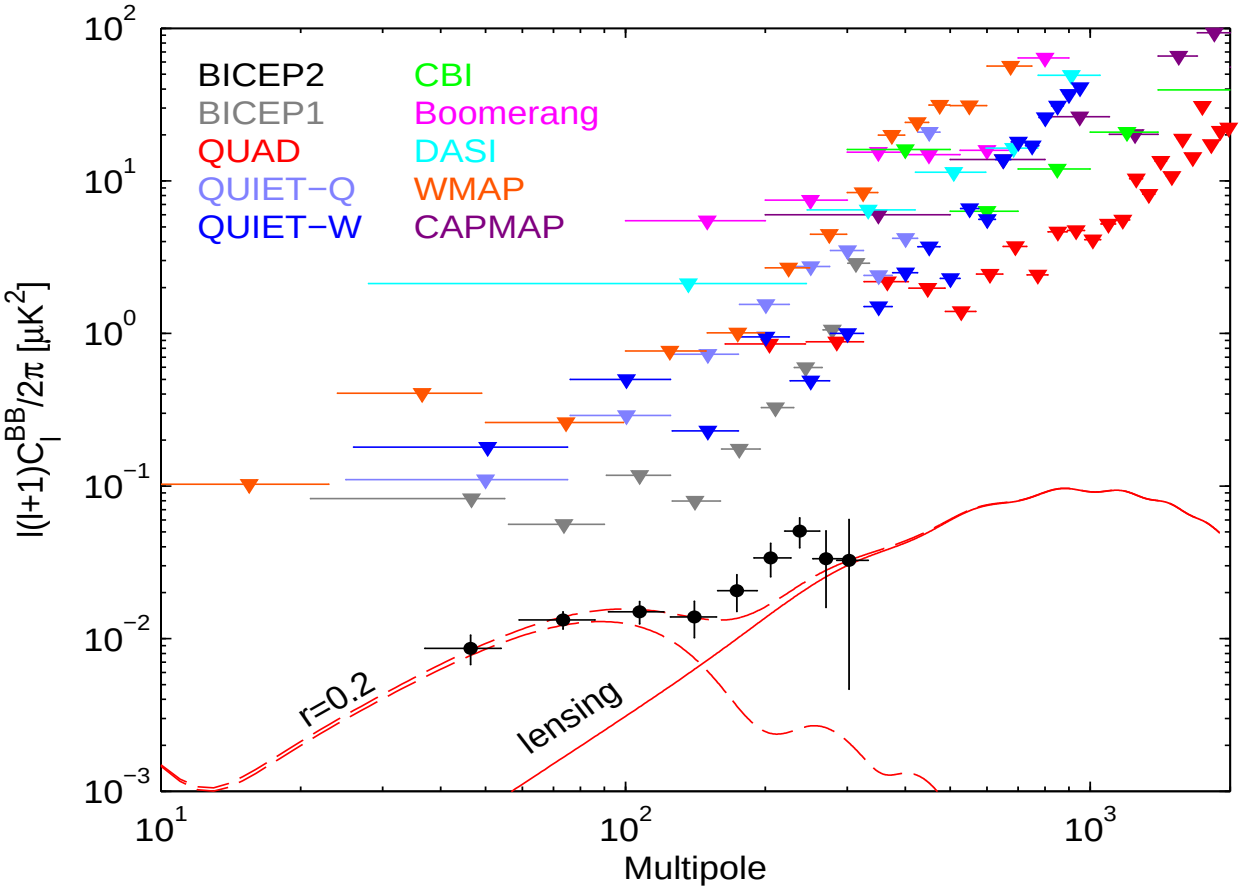

The detection of the angular power spectrum of the B-mode polarization of the CMB by BICEP2 as well as the limits that have been arrived at by the earlier efforts[20]. The BICEP2 observations, *viz.* the black dots with error bars, seem to be consistent with a tensor-to-scalar ratio of $r \simeq 0.2$.

[20] P. A. R. Ade *et al.*, arXiv:1403.3985 [astro-ph.CO].

Inflation resolves the horizon problem

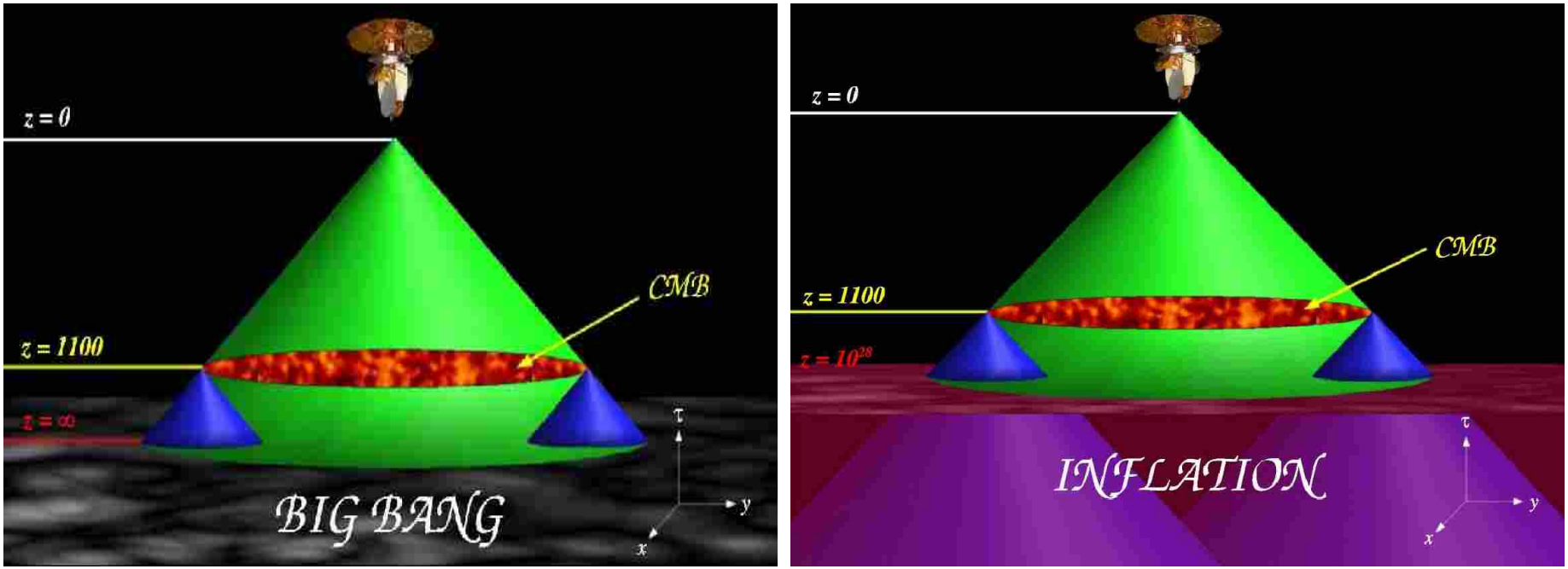

Left: The radiation from the CMB arriving at us from regions separated by more than the Hubble radius at the last scattering surface (which subtends an angle of about 1° today) could not have interacted before decoupling.
Right: An illustration of how an early and sufficiently long epoch of inflation helps in resolving the horizon problem[21].

[21] Images from W. Kinney, astro-ph/0301448.

Bringing the modes inside the Hubble radius

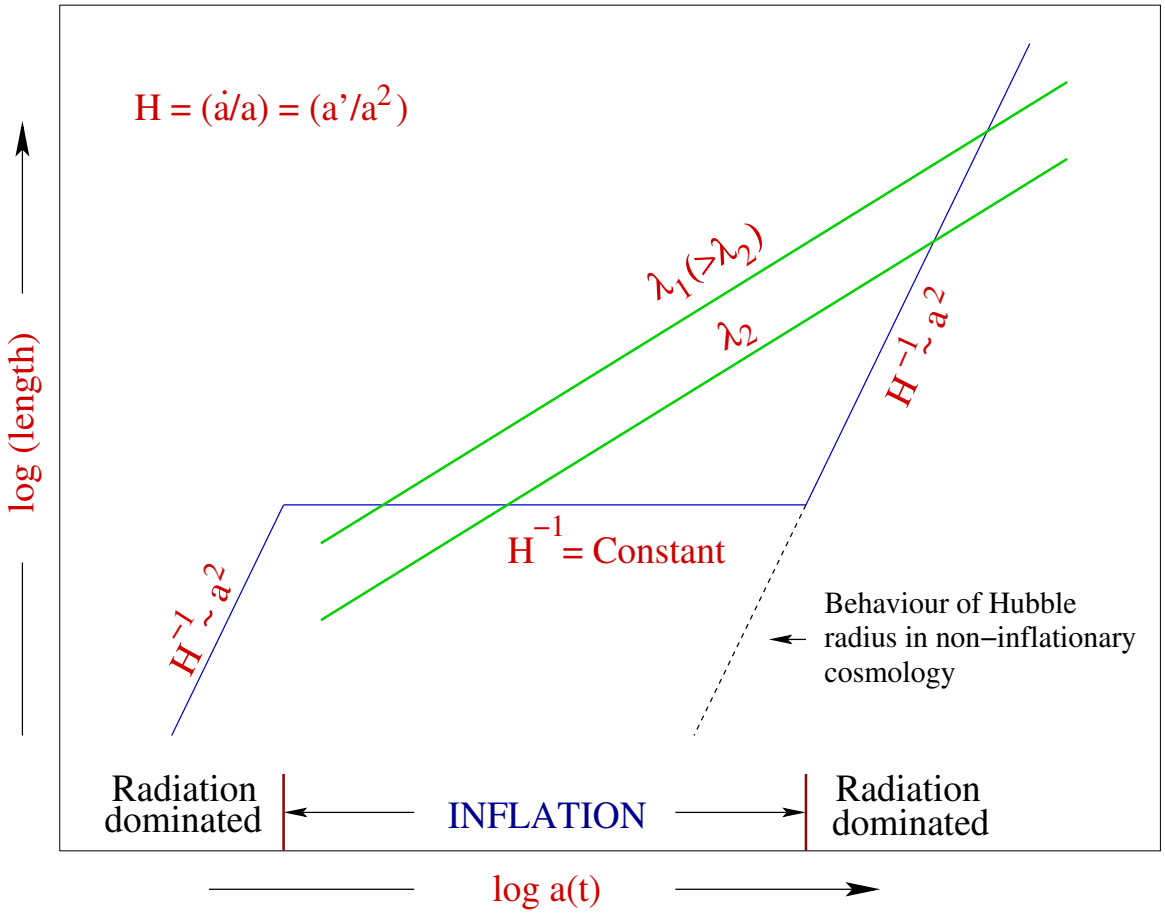

A schematic diagram illustrating the behavior of the physical wavelength $\lambda_{\rm P} \propto a$ (the green lines) and the Hubble radius $d_{\rm H} = H^{-1}$ (the blue line) during inflation and the radiation dominated epochs[22].

[22] See, for example, E. W. Kolb and M. S. Turner, *The Early Universe* (Addison-Wesley Publishing Company, New York, 1990), Fig. 8.4.

Necessary conditions for inflation

If we require that $\lambda_{\rm P} < d_{\rm H}$ at a sufficiently early time, then we need to have an epoch wherein $\lambda_{\rm P}$ decreases faster than the Hubble scale *as we go back in time*, *i.e.* a regime during which[23]

$$-\frac{\mathrm{d}}{\mathrm{d}t}\left(\frac{\lambda_{\rm P}}{d_{\rm H}}\right) < 0 \quad \Rightarrow \quad \ddot{a} > 0.$$

From the Friedmann equations, we have

$$\frac{\ddot{a}}{a} = -\frac{4\,\pi\,G}{3}\,(\rho + 3\,p)\,.$$

Evidently, $\ddot{a} > 0$ when

$$\rho + 3\,p < 0.$$

[23] See, for example, L. Sriramkumar, Curr. Sci. **97**, 868 (2009).

Scalar fields can drive inflation[24]

In a smooth Friedmann universe, the energy density ρ and pressure p corresponding to a homogeneous and canonical scalar field, say, ϕ, that is described by the potential $V(\phi)$, are given by

$$\rho = \frac{\dot{\phi}^2}{2} + V(\phi) \quad \text{and} \quad p = \frac{\dot{\phi}^2}{2} - V(\phi).$$

The scalar field satisfies the following equation of motion:

$$\ddot{\phi} + 3\,H\,\dot{\phi} = -V_{\phi}, \quad \text{where} \quad V_{\phi} \equiv \mathrm{d}V/\mathrm{d}\phi.$$

In such a case, the condition $\rho + 3\,p < 0$ simplifies to

$$\dot{\phi}^2 < V(\phi).$$

This condition can be achieved if the scalar field ϕ is initially displaced from a minima of the potential, and inflation will end when the field approaches a minima with zero or negligible potential energy.

[24] See, for instance, L. Sriramkumar, Curr. Sci. **97**, 868 (2009).

A variety of potentials to choose from

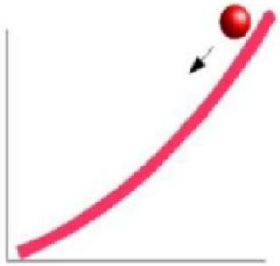

Large_field

$$V(\phi) = \Lambda^4 (\phi/\mu)^p$$

$$V(\phi) = \Lambda^4 e^{\phi/\mu}$$

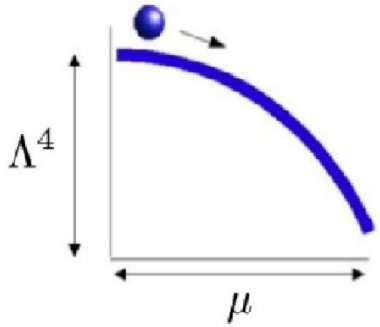

Small_field

$$V(\phi) = \Lambda^4 [1 - (\phi/\mu)^p]$$

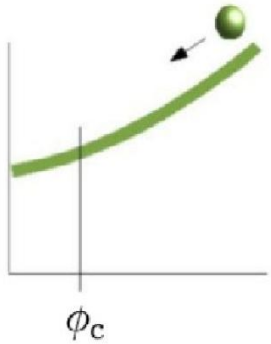

Hybrid

$$V(\phi) = \Lambda^4 [1 + (\phi/\mu)^p]$$

A variety of scalar field potentials have been considered to drive inflation[25]. Often, these potentials are classified as small field, large field and hybrid models.

[25] Image from W. Kinney, astro-ph/0301448.

The inflationary perturbation spectra

The curvature and the tensor perturbations, say, $\mathcal{R}_k$ and $\mathcal{U}_k$, satisfy the differential equations

$$\mathcal{R}_k'' + 2\,(z'/z)\,\mathcal{R}_k' + k^2\,\mathcal{R}_k = 0 \quad \text{and} \quad \mathcal{U}_k'' + 2\,\mathcal{H}\,\mathcal{U}_k' + k^2\,\mathcal{U}_k = 0,$$

where $z = a\,\phi'/\mathcal{H}$, with ϕ denoting the background inflaton, and $\mathcal{H} = a'/a$ is the conformal Hubble parameter[26].

The inflationary scalar and tensor power spectra, *viz.* $\mathcal{P}_{\rm S}(k)$ and $\mathcal{P}_{\rm T}(k)$, are defined as

$$\mathcal{P}_{\rm S}(k) = \frac{k^3}{2\,\pi^2}\,|\mathcal{R}_{\rm k}|^2 \quad \text{and} \quad \mathcal{P}_{\rm T}(k) = 4\,\frac{k^3}{2\pi^2}\,|\mathcal{U}_{\rm k}|^2,$$

with the amplitudes $\mathcal{R}_k$ and $\mathcal{U}_k$ evaluated, in general, in the super-Hubble limit.

As we have already seen, the tensor-to-scalar ratio r is given by

$$r(k) \equiv \frac{\mathcal{P}_{\rm T}(k)}{\mathcal{P}_{\rm S}(k)}.$$

[26] See, for instance, B. A. Bassett, S. Tsujikawa and D. Wands, Rev. Mod. Phys. **78**, 537 (2006).

The spectral indices and their running

The scalar spectral index and its running are defined as[27]

$$n_{\rm S} \equiv 1 + \frac{{\rm d}\ln \mathcal{P}_{\rm S}}{{\rm d}\ln k} \quad \text{and} \quad \alpha_{\rm S} \equiv \frac{{\rm d}\, n_{\rm S}}{{\rm d}\ln k}.$$

Whereas, the tensor spectral index and its running are given by

$$n_{\rm T} \equiv \frac{{\rm d}\ln \mathcal{P}_{\rm T}}{{\rm d}\ln k} \quad \text{and} \quad \alpha_{\rm T} \equiv \frac{{\rm d}\, n_{\rm T}}{{\rm d}\ln k}.$$

[27] See B. A. Bassett, S. Tsujikawa and D. Wands, Rev. Mod. Phys. **78**, 537 (2006).

The slow roll approximation

Given a potential $V(\phi)$, the slow roll approximation requires that the following *potential* slow roll parameters be small when compared to unity[28]:

$$\epsilon_{\rm V} = \frac{\rm M_{Pl}^2}{2}\left(\frac{V_\phi}{V}\right)^2 , \quad \eta_{\rm V} = \rm M_{Pl}^2\left(\frac{V_{\phi\phi}}{V}\right) \quad \text{and} \quad \xi^2 = \rm M_{Pl}^4\left(\frac{V_\phi\, V_{\phi\phi\phi}}{V^2}\right) ,$$

where $V_{\phi\phi} \equiv \mathrm{d}^2V/\mathrm{d}\phi^2$ and $V_{\phi\phi\phi} \equiv \mathrm{d}^3V/\mathrm{d}\phi^3$. Note that the smallness of the parameters $\epsilon_{\rm V}$ and $\eta_{\rm V}$ is a *sufficient* condition for inflation to occur, and inflation ends when $\epsilon_{\rm V} = 1$.

Nowadays, it is more common to use the following hierarchy of Hubble flow functions[29]:

$$\epsilon_1 \equiv -\frac{\dot{H}}{H^2} \quad \text{and} \quad \epsilon_{i+1} \equiv \frac{\mathrm{d}\ln|\epsilon_i|}{\mathrm{d}N} \quad \text{for} \quad i \geq 1 ,$$

with H_* being the Hubble parameter evaluated at some given time.

[28] See, for instance, A. R. Liddle, P. Parsons and J. D. Barrow, Phys. Rev. D **50**, 7222 (1994).

[29] D. J. Schwarz, C. A. Terrero-Escalante, A. A. Garcia, Phys. Lett. B **517**, 243 (2001); S. M. Leach, A. R. Liddle, J. Martin and D. J. Schwarz, Phys. Rev. D **66**, 023515 (2002).

The slow roll scalar amplitude, index and running[30]

At the leading order in the slow roll approximation, the spectral amplitude of the curvature perturbation can be expressed in terms of the potential $V(\phi)$ as follows:

$$\mathcal{P}_{\rm S}(k) \simeq \frac{1}{12\,\pi^2\,{\rm M}_{\rm Pl}^6}\left(\frac{V^3}{V_\phi^2}\right)_{k=a\,H}$$

with the subscript on the right hand side indicating that the quantity has to be evaluated when the modes leave the Hubble radius.

At the same order of the approximation, the scalar spectral index is given by

$$n_{\rm S} \equiv 1 + \left(\frac{{\rm d}\ln\mathcal{P}_{\rm S}}{{\rm d}\ln k}\right)_{k=a\,H} = 1 - 2\,\epsilon_1 - \epsilon_2\,,$$

while the running of the scalar spectral index can be evaluated to be

$$\alpha_{\rm S} \equiv \left(\frac{{\rm d}\,n_{\rm S}}{{\rm d}\ln k}\right)_{k=a\,H} = -\left(2\,\epsilon_1\,\epsilon_2 + \epsilon_2\,\epsilon_3\right)\,.$$

[30] See, for instance, B. A. Bassett, S. Tsujikawa and D. Wands, Rev. Mod. Phys. **78**, 537 (2006).

The tensor amplitude, spectral index and running

At the leading order in the slow roll approximation, the tensor amplitude is given by

$$\mathcal{P}_{\rm T}(k) \simeq \frac{2}{3\,\pi^2}\,\left(\frac{V}{{\rm M}_{\rm Pl}^4}\right)_{k=a\,H},$$

while the spectral index and the running can be estimated to be[31]

$$n_{\rm T} \equiv \left(\frac{{\rm d}\ln\mathcal{P}_{\rm T}}{{\rm d}\ln k}\right)_{k=a\,H} = -2\,\epsilon_1 \quad \text{and} \quad \alpha_{\rm T} \equiv \left(\frac{{\rm d}\,n_{\rm T}}{{\rm d}\ln k}\right)_{k=a\,H} = -2\,\epsilon_1\,\epsilon_2.$$

The tensor-to-scalar ratio is then given by

$$r \equiv \frac{\mathcal{P}_{\rm T}(k)}{\mathcal{P}_{\rm S}(k)} \simeq 16\,\epsilon_1 = -8\,n_{\rm T},$$

with the last equality often referred to as the consistency relation[32].

[31] See, B. A. Bassett, S. Tsujikawa and D. Wands, Rev. Mod. Phys. **78**, 537 (2006).

[32] J. E. Lidsey, A. R. Liddle, E. W. Kolb and E. J. Copeland, Rev. Mod. Phys. **69**, 373 (1997).

Classification of inflation models in the $n_{\rm S}$-r plane[33]

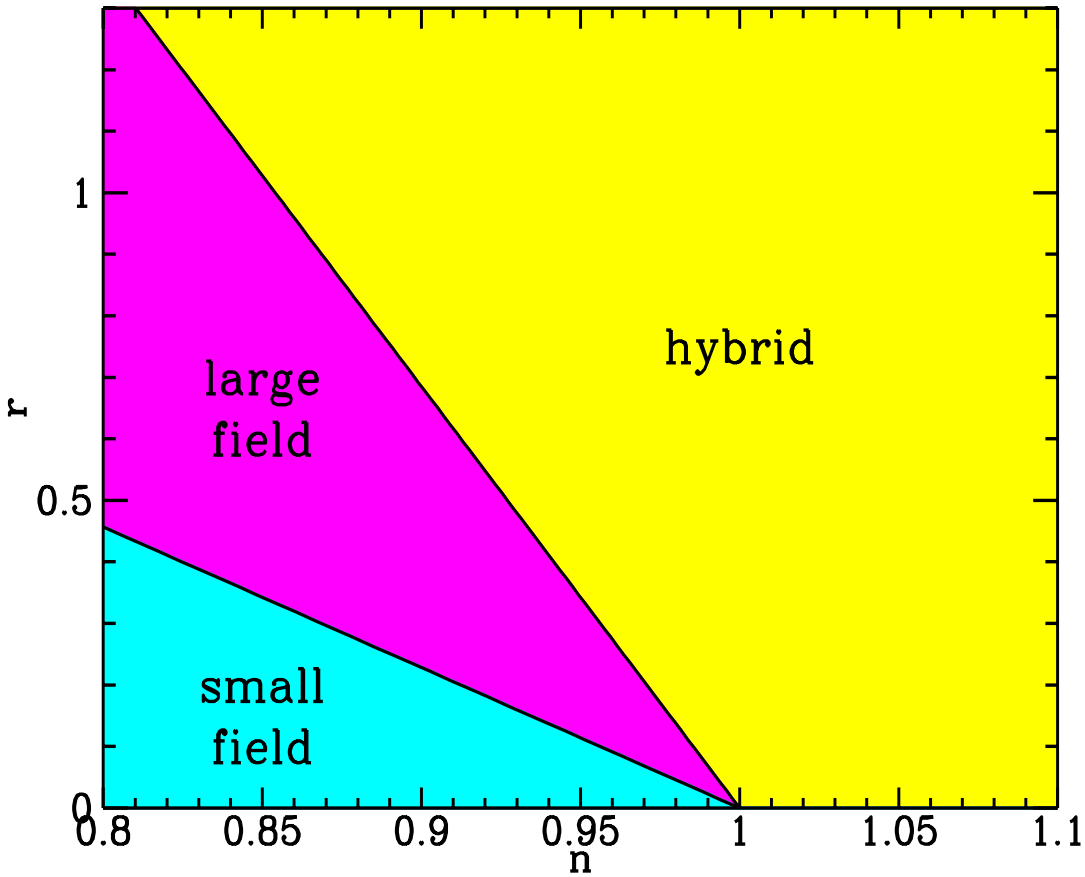

The potential $V(\phi) \propto \phi$ separates the small field ($\eta_{\rm V} < 0$) and large field models ($0 < \eta_{\rm V} \leq 2\,\epsilon_{\rm V}$), while the exponential potential $V(\phi) \propto \exp -[\sqrt{2/\alpha}\,(\phi/{\rm M_{Pl}})]$ divides the large field models from the hybrid ones ($\eta_{\rm V} > 2\,\epsilon_{\rm V}$).

[33] Figure from W. H. Kinney, A. Melchiorri and A. Riotto, Phys. Rev. D **63**, 023505 (2001).

Constraints from the WMAP data[34]

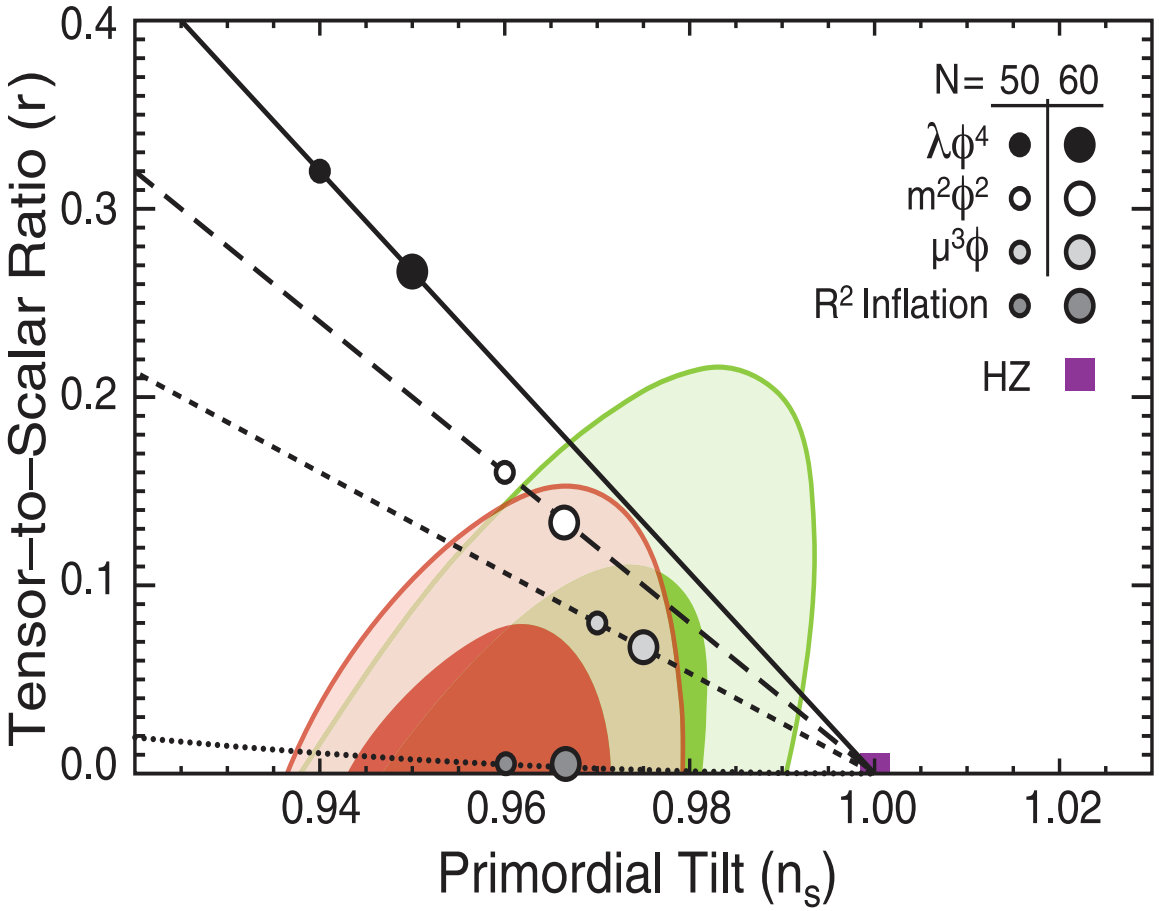

Joint constraints from the WMAP nine-year and other cosmological data on the inflationary parameters $n_{\rm S}$ and r for large field models with potentials of the form $V(\phi) \propto \phi^n$.

[34] G. Hinshaw *et al.*, Astrophys. J. Suppl. **208**, 19 (2103).

Constraints from Planck[35]

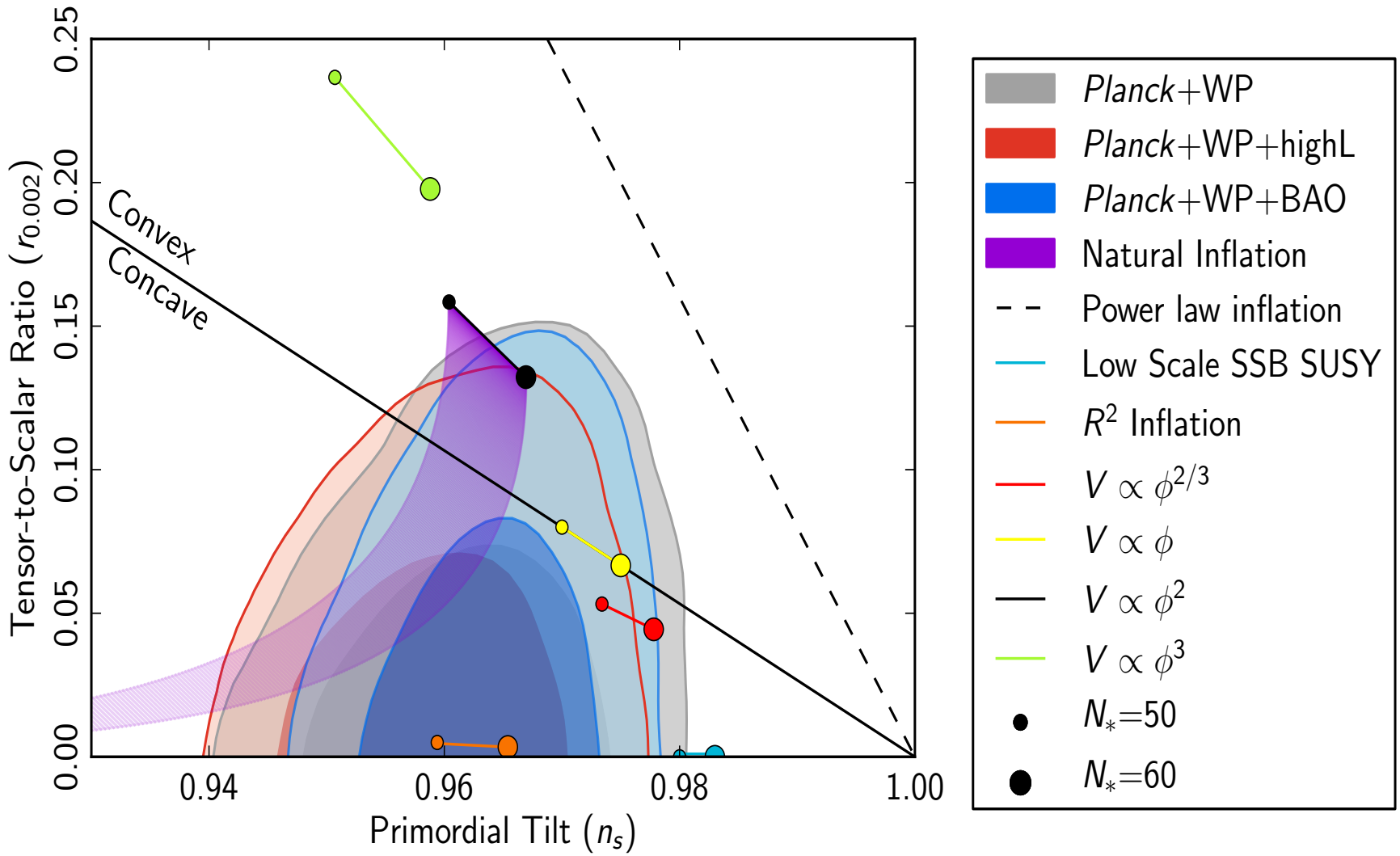

The corresponding constraints from the Planck data for various models.

[35] P. A. R. Ade *et al.*, arXiv:1303.5082 [astro-ph.CO].

Constraints from the BICEP2 data[36]

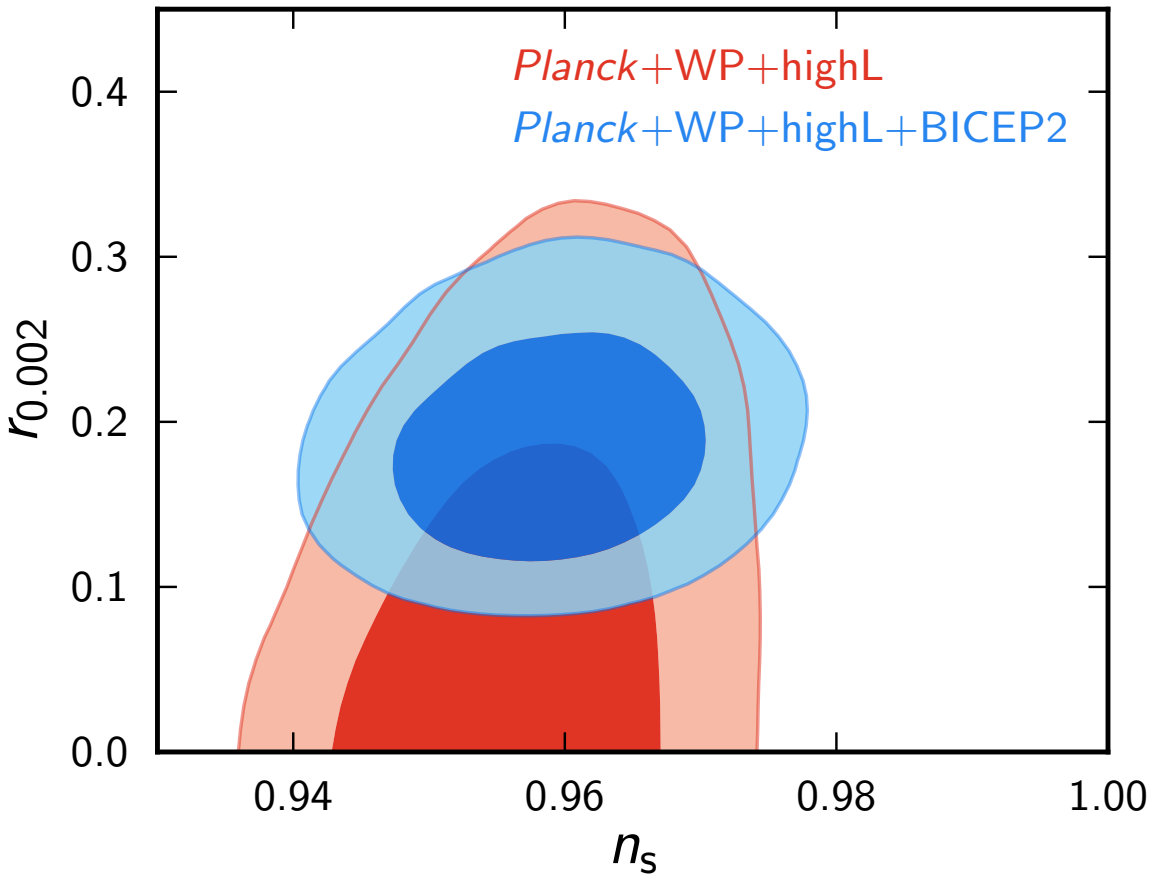

Joint constraints from the BICEP2 observations and the Planck data as well as the polarization data from WMAP on the inflationary parameters $n_{\rm S}$ and r. The tensor-to-scalar ratio is determined to be $r = 0.20^{+0.07}_{-0.05}$, with $r = 0$ being ruled out at 7-σ!

[36] P. A. R. Ade *et al.*, arXiv:1403.3985 [astro-ph.CO].

Performance of inflationary models

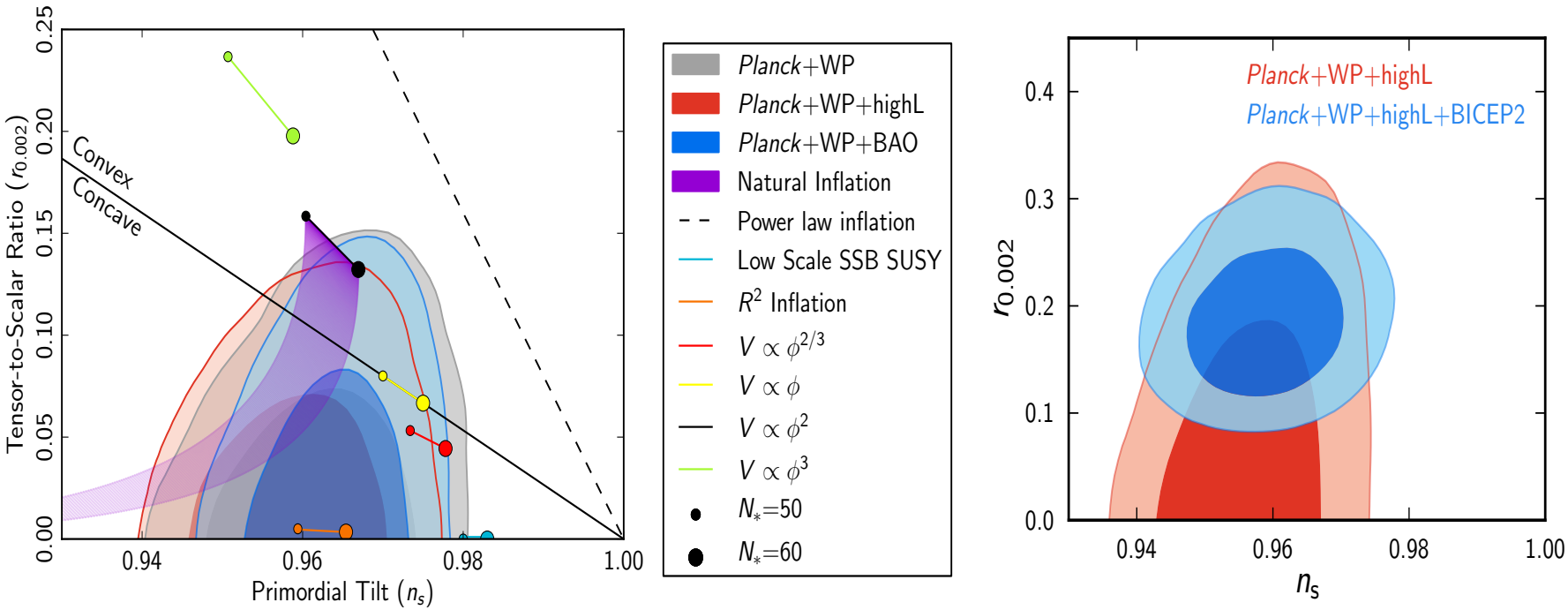

The constraints on inflationary models from the Planck data (on the left) and the joint constraints in the n_s-r plane from the BICEP2 observations (on the right) have been illustrated together to gain an understanding of the performance of the models against the new data.

Amazing prescience!

VOLUME 78, NUMBER 10 PHYSICAL REVIEW LETTERS 10 MARCH 1997

What Would We Learn by Detecting a Gravitational Wave Signal in the Cosmic Microwave Background Anisotropy?

David H. Lyth

School of Physics and Chemistry, Lancaster University, Lancaster LA1 4YB, United Kingdom

(Received 20 June 1996)

Inflation generates gravitational waves, which may be observable in the low multipoles of the cosmic microwave background anisotropy but only if the inflaton field variation is at least of order the Planck scale. Such a large variation would imply that the model of inflation cannot be part of an ordinary extension of the standard model, and combined with the detection of the waves it would also suggest that the inflaton field cannot be one of the superstring moduli. Another implication of observable gravitational waves would be a potential $V^{1/4} = 2$ to 4×10^{16} GeV , which is orders of magnitude bigger than the prediction of most models. [S0031-9007(97)02506-4]

PACS numbers: 98.80.Cq, 04.30.Db, 98.70.Vc

A paper by David Lyth from 1997 with a title that seems amazingly apt in the light of BICEP2 observations.

The scale of inflation

During slow roll, if we ignore the weak scale-dependence, we can write

$$r \simeq \frac{2\,V}{3\,\pi^2\,\mathrm{M}_{\mathrm{Pl}}^4}\,\frac{1}{\mathcal{A}_{\mathrm{S}}},$$

where, recall that, $\mathcal{A}_{\mathrm{S}}$ denotes the amplitude of the scalar perturbations.

The amplitude of the primordial scalar perturbations is usually quoted at the pivot scales of either 0.05 or $0.02\,\mathrm{Mpc}^{-1}$, which correspond to multipoles that lie in the Sachs-Wolfe plateau. This value for the scalar amplitude is often referred to as COBE normalization[37].

According to COBE normalization, $\mathcal{A}_{\mathrm{S}} \simeq 2.14 \times 10^{-9}$, which implies that we can write

$$V^{1/4} \simeq 3.2 \times 10^{16}\, r^{1/4}\,\mathrm{GeV} \simeq 2.1 \times 10^{16}\,\mathrm{GeV},$$

with the final value being for the case wherein $r \simeq 0.2$.

Note that, if H_{I} represents the Hubble scale during inflation, as $H_{\mathrm{I}}^2 \simeq V/\mathrm{M}_{\mathrm{Pl}}^2$ during slow roll, the above relation also leads to

$$\frac{H_{\mathrm{I}}}{\mathrm{M}_{\mathrm{Pl}}} \simeq 8.0 \times 10^{-5}.$$

[37] E. F. Bunn, A. R. Liddle and M. J. White, Phys. Rev. D **54**, R5917 (1996).

The Lyth bound

Gravitational waves are expected to decay once they enter the Hubble radius during the radiation or the matter dominated epochs.

As a result, the contributions of the primordial gravitational waves to the B-mode of the CMB polarization angular power spectrum drops sharply after multipoles of $\ell \simeq 100$, roughly around the same multipoles where the TT angular power spectrum exhibits its first peak.

The CMB quadrupole, *i.e.* $\ell = 2$, corresponds to the largest cosmological scale of interest, *viz.* the Hubble radius H_0^{-1} today. Hence, we can relate the wavenumbers to the multipoles as $k \simeq H_0\,\ell/2$. Therefore, a Δl corresponds to the width $\Delta k \simeq H_0\,\Delta\ell/2$ in terms of wavenumbers.

As $a \propto \mathrm{e}^N$, the modes over a domain Δk corresponding to $\Delta l \simeq 100$ will leave the Hubble radius during inflation over the time period $\Delta N \simeq \log 100 \simeq 3.9$.

During slow roll, we have $H^2 = V/(3\,\mathrm{M}_{\mathrm{Pl}}^2)$ and $3\,H\,\dot{\phi} \simeq V_\phi$, so that[38]

$$\Delta\phi \simeq (r/8)^{1/2}\,\Delta N\,\mathrm{M}_{\mathrm{Pl}} \simeq 0.6\,\mathrm{M}_{\mathrm{Pl}},$$

with the final value corresponding to $r \simeq 0.2$.

[38] D. H. Lyth, Phys. Rev. Letts. **78**, 1861 (1997).

Summary

- BICEP2 has detected the B-mode polarization of the CMB angular power spectrum at large angular scales corresponding to the multipoles of $30 \lesssim \ell \lesssim 150$.
- These multipoles correspond to cosmological scales and, hence, the observations are signatures of primordial gravitational waves.
- The observations of BICEP2 correspond to a rather high tensor-to-scalar ratio of $r \simeq 0.2$. Importantly, the BICEP2 team concludes that a vanishing tensor-to-scalar ratio is ruled out at 7-σ.
- If inflation is indeed the mechanism that had generated these primordial gravitational waves, it implies that inflation had occurred at an energy scale of $V^{1/4} \simeq 2.1 \times 10^{16}\,\mathrm{GeV}$. Also, the inflaton would have rolled over $\Delta\phi \simeq 0.6\,\mathrm{M_{Pl}}$ in order to generate the observed amplitude of the tensor modes.
- However, there seems to exist some tension between the BICEP2 observations and the Planck data, which may require to be resolved (say, by BICEP3), before the last word can possibly be said.

Thank you for your attention